

Deep learning regression for inverse quantum scattering

A. C. Maioli*

(Dated: September 22, 2020)

In this work we study the inverse quantum scattering via deep learning regression, which is implemented via a Multilayer Perceptron. A step-by-step method is provided in order to obtain the potential parameters. A circular boundary-wall potential was chosen to exemplify the method. Detailed discussion about the training is provided. An investigation with noisy data is presented and it is observed that the neural network is useful to predict the potential parameters.

I. INTRODUCTION

Machine Learning is a collection of powerful tools that predicts parameters or classify features based on experimental or synthetic data. A plethora of applications exist, such as the reconstruction of porous media [1], feature selection by mutual information [2], percolation and fracture propagation in disordered solids [3], the behavior of Ising spin-lattice [4], a model for turbulent fluxes that recovers spontaneous zonal flow [5], classification of complex features in diffraction images [6] and much more [7–9].

Recently, two-dimensional quantum scattering is receiving attention, E. de Prunel gave a formulation for non-isotropic interactions localized on circle [10]. Maioli *et al* found analytic solutions for the wavefunction scattered by circular and elliptic billiards [11, 12] and presented a scattering with two-potential formalism [13]. Which they used a boundary-wall potential introduced by M. G. E. da Luz *et al* [14]. Therefore, F. M Zanetti *et al* explores the eigenstates and scattering solutions for billiards using the Boundary Wall Method (BWM) [15], which is useful to find analytic solutions for the T matrix. Along these lines, the BWM provides a significant way to study quantum scattering and electromagnetic wave propagation for TE or TM modes due to the analogy of both physical phenomena [16]. On the other hand, inverse scattering problems have a significant role in applied physics, such as the reconstruction of medium properties [17]. In this scenario, G. Ariel and H. Diamant [18] shown a method to infer the entropy from the structure factor (which can be obtained by quantum scattering), and T. Tyni numerically investigated the two-dimensional inverse scattering with the aid of Saito's uniqueness theorem [19]. G. Fotopoulos and M. Harju [20] study how to retrieve the singularities of a unknown potential using the Born approximation.

The goal of this work is to provide a simple method that obtains the potential parameters based on the scattering data. This type of inverse problem is extensively frequent in scattering physics. It is designated a regression problem in the machine learning vocabulary. The method consists in choosing a potential that model the physical system, then generate synthetic data to train

a neural network. In order to employ the method we choose the circular boundary wall potential. Employ a neural network to solve a regression problem is considered exceedingly good, and the results improve as one adds more hidden layers. However, it can be computationally exhaustive and hard to converge the network's parameters due to the vanishing gradient problem. Therefore we show how to avoid the last difficulty. The trained neural network can predict the correct results even when the input data has noise and the training set doesn't.

This paper is organized as follows. In Section II we present the method detailed, including how the synthetic data was generated (subsection II B) and the neural network training (subsection II D). In section III, it is shown that the trained neural network can predict the correct values for the potential parameters. Finally we conclude the discussions on section IV.

II. THE METHOD

The main idea is to provide a fast way to find the potential parameters due to the scattering cross length $l(k)$ obtained for the two-dimensional quantum scattering. The scattering cross length is the two-dimensional analogs of the scattering cross-section, the usual formulation can be found at [21–23] and a comparison between 2D and 3D formulas [24]. The method embraces a few simple steps, and some hints follow the example selected throughout this work. The steps are:

1. Choose the potential that suits the desired physical system.
2. Generate synthetic data that will be the input of the neural network. One can use the scattering cross length and other physical information, such as particle's mass, Plank's constant, etc. There is no need to worry about noise at this step. Therefore, the output is the potential parameters.
3. Build a neural network. The size of the input will be the number of physical quantities necessary to perform the regression.
4. Train the neural network with synthetic data.

* alanmaioli90@gmail.com

A. First Step: Boundary wall potential

Here we use a circular boundary-wall potential that is defined as a line integral

$$V(\mathbf{r}) = \int_C \gamma(s) \delta^2(\mathbf{r} - \mathbf{r}(s)) ds, \quad (1)$$

where $\gamma(s)$ is the strength function, which we set to be constant $\gamma(s) = \gamma_0$, C is a circle of radius R , the δ^2 is the two-dimensional Dirac delta. Writing the potential as a

$$\psi(\mathbf{r}) = J_0(kr) + u_0 H_0^{(1)}(kr) + 2 \sum_{n=1}^{\infty} i^n \left[J_n(kr) + u_n H_n^{(1)}(kr) \right] \cos [n(\theta + (-1)^n \alpha)], \quad (3)$$

where J_n and $H_n^{(1)}$ are the Bessel and Hankel function of the first kind of order n , respectively, α is the angle between the wave vector \mathbf{k} of the plane wave and the x -axis, and

$$u_n = \frac{2\pi R \gamma \sigma J_n^2(kR)}{1 - 2\pi R \gamma \sigma J_n(kR) H_n^{(1)}(kR)}, \quad (4)$$

where $\sigma = (-i/4)(2m/\hbar^2)$. For the sake of simplicity, we set $\alpha = 0$, then using the relation $i^n J_n(kr) = i^{-n} J_{-n}(kr)$ and $i^n H_n^{(1)}(kr) = i^{-n} H_{-n}^{(1)}(kr)$ one can rewrite the eq. (3)

$$\psi(\mathbf{r}) = e^{ikx} + \sum_{n=-\infty}^{\infty} i^n u_n H_n^{(1)}(kr) e^{in\theta}, \quad (5)$$

where the sum of Bessel functions was identified as the exponential. Along these lines, one can use the asymptotic expansion of the Hankel function

$$H_n^{(1)}(kr) \approx \sqrt{\frac{2}{\pi k}} e^{-i\pi/4} e^{ikr} e^{-in\theta/2}, \quad (6)$$

then it is easy to find the scattering amplitude $f(\theta)$ using

$$\psi(\mathbf{r}) \approx e^{ikx} + \frac{e^{ikr}}{\sqrt{r}} f(\theta), \quad (7)$$

therefore

$$f(\theta) = \sqrt{\frac{2}{\pi k}} e^{-i\pi/4} \sum_{n=-\infty}^{\infty} u_n e^{in\theta}. \quad (8)$$

Riemann integral, we have

$$V(\mathbf{r}) = \gamma R \int_{-\pi}^{\pi} \frac{\delta(\mathbf{r} - R) \delta(\theta - s)}{r} ds, \quad (2)$$

one can see that the parameters γ and R uniquely define this type of potential, therefore those are the ones which we need to predict.

B. Second step: Synthetic data

In this subsection is presented an expression for the scattering cross length $l(k)$. It will be employed to generate the synthetic data. Therefore, it is obtained through the analytic solution of the Lippmann-Schwinger equation outside the circle ($r > R$) [11],

For central potentials it is useful to apply the partial wave analysis,

$$f(\theta) = \sum_{l=-\infty}^{\infty} f_l e^{il\theta}, \quad (9)$$

where

$$f_l = \sqrt{\frac{2}{\pi}} e^{i\pi/4} \sqrt{\frac{1}{k}} e^{i\delta_n} \sin \delta_n, \quad (10)$$

and δ_n is the phase shift. One can find an analytic expression for the phase shift after combining eq. (8), (9) and (10)

$$\delta_n = \frac{\log(1 + 2u_n)}{2i}, \quad (11)$$

and a relation for the scattering cross length

$$l(k) = \frac{4}{k} \sum_{n=-\infty}^{\infty} \sin^2(\delta_n) = -\frac{4}{k} \sum_{n=-\infty}^{\infty} \text{Re}[u_n], \quad (12)$$

where $\text{Re}[u_n]$ stands for the Real part of u_n .

1. Data Detailed

For a chosen γ and R it is computed $l(k)$ for several values of k . It begins with $k_{min} = 0.02$ and ends at $k_{max} = 3$ with increments $\Delta k = 0.005$, and it is used natural units $m = \hbar = 1$. The series of eq. (12) was truncated at $n_{max} = 20$

$$l(k) = -\frac{4}{k} \sum_{n=-20}^{20} \text{Re}[u_n]. \quad (13)$$

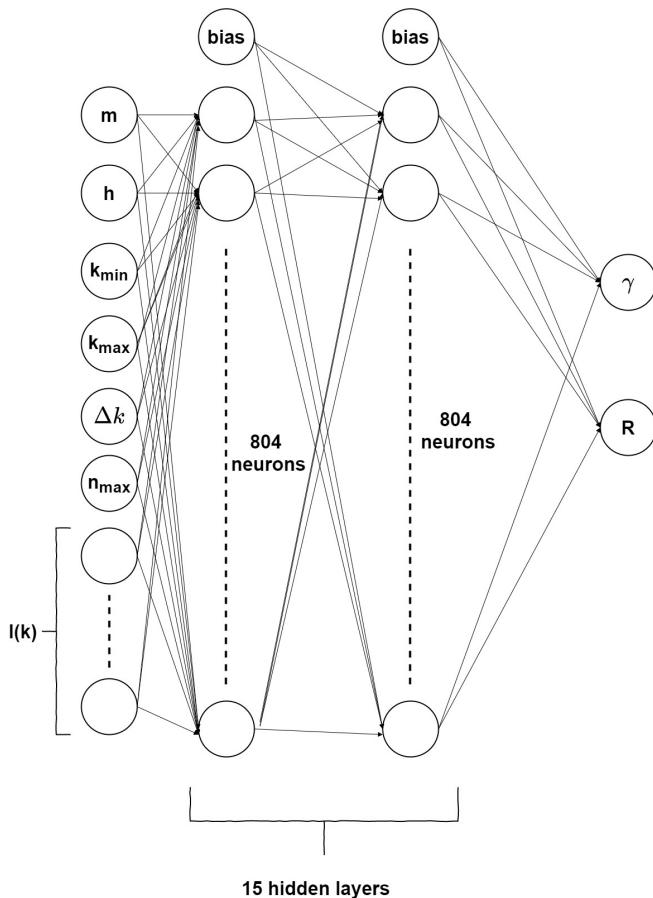


FIG. 1. A schematic representation of the neural network. The input have 603 values, which is defined by $\mathbf{x} = (m, h, k_{min}, k_{max}, \Delta k, n_{max}, l(k_{min}), \dots, l(k_{max}))^T$. The output contains two values R and γ . Each hidden layer has 804 neurons, and there are 15 hidden layers.

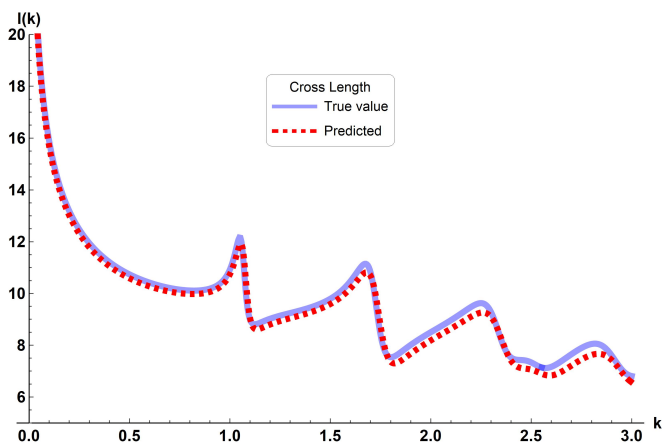


FIG. 2. Plot of the scattering cross length. The blue (gray) full line is related to the true values $R = 2$ and $\gamma = 2$, and the red (black) dashed line to the “predicted” values $\gamma \approx 1.92$ and $R \approx 1.98$ obtained via the trained neural network.

So, one synthetic data is the group of 603 values $\mathbf{x} = (m, h, k_{min}, k_{max}, \Delta k, n_{max}, l(k_{min}), \dots, l(k_{max}))^T$. Those values are organized as a column vector \mathbf{x} and are the input of the neural network. Therefore, we generate 55100 synthetic data, for different values of R and γ , where R spans from 0.1 to 2 with steps of 0.01, and γ from 0.1 to 3 with increment 0.01.

C. Third Step: Build a neural network

Choose a specific Neural Network to implement a regression problem is a decisive matter due to the antagonism between the computational time to execute the program and the spend personal time desired to obtain the solution. Among several types of Neural Networks (such as Recurrent Neural Network, Modular Neural Network, Convolutional Neural Network, and some more), we choose a Multilayer Perceptron because it has a simple set-up and provides excellent results. The number of hidden layers in this work (15) is justified at the subsection IID. Usually, the more hidden layer in the network better is the results, until it starts to overfitting. However, for hidden neurons, one may use some rules:

- The number of hidden neurons should be between the size of the input layer and the size of the output layer.
- The number of hidden neurons should be 2/3 the size of the input layer, plus the size of the output layer.
- The number of hidden neurons should be less than twice the size of the input layer.

Those rule-of-thumbs appear at [25]. The chosen number in this example was the size of the input plus one-third of it (804), and the activation function was the logistic sigmoid.

D. Fourth Step: The Training

In order to train the neural network, the synthetic data was randomly separated among three groups, namely training set, validation set and test set. The test set has 20% of the total number of the synthetic data. The remaining (80%) was allocated between the training set and validation set. 30% of it for the validation set and 70% to the training set. This separation is important to check the accuracy of the network. The error (loss or cost) function J employed is the mean squared difference

$$J(\mathbf{y}, \mathbf{y}') = \frac{1}{N} \sum_{j=1}^N (y_j - y'_j)^2, \quad (14)$$

where $\mathbf{y} = (y_1, \dots, y_N)^T$ is the network output, $N = 2$ is the size of the output and $\mathbf{y}' = (y'_1, \dots, y'_N)^T$ is the desired

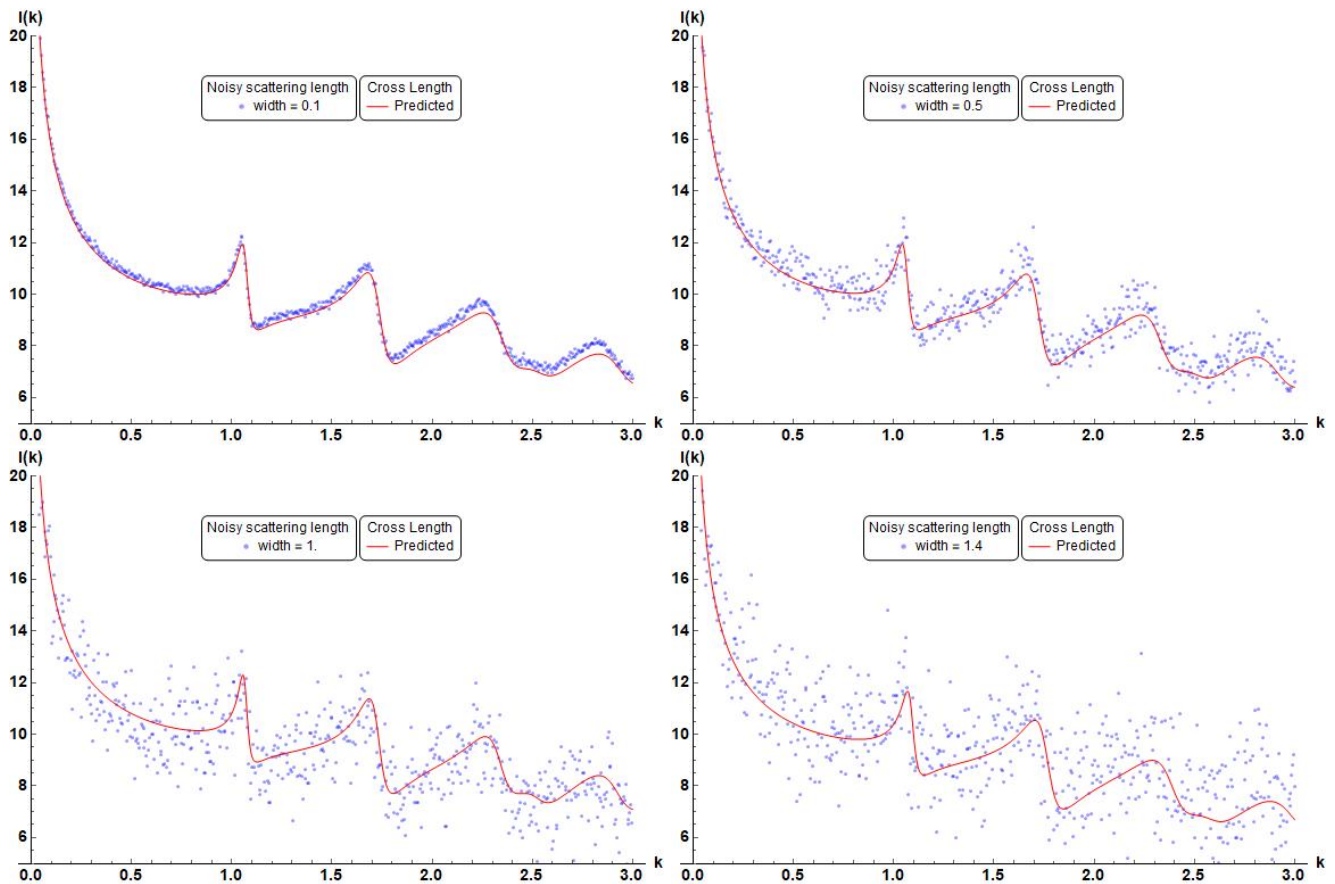


FIG. 3. Scatter plot of the noisy scattering cross length with noise width $w = 0.1$ (upper left), $w = 0.5$ (upper right), $w = 1.0$ (bottom left), $w = 1.4$ (bottom right). The red full line correspond to the scattering cross length calculated with the predicted parameters obtained via the trained neural network.

output, in other words, the γ and R used to produce \mathbf{x} . The training method is the stochastic gradient descent with a batch size of 100 examples, where is important to apply an adaptive learning rate that is invariant to diagonal rescaling of the gradients. However, one should avoid train the neural network directly, because of the vanishing gradient problem. This leads to a network with high bias.

It is known, that a cascade-correlation learning architecture [26] solves this problem. The procedure consists in training the network several times, first with only one hidden layer. Then, one adds another hidden layer and keep the weights learned previously. At each training, one must check the convergence of the error over the test set, the validation set. If the error calculated over the validation set increases (over each iteration at one training), then you have overfitting. To solve this problem decrease the number of hidden neurons. Finally, it is imperative to apply the network over the test set at the end of each training, because one can visualize the error decreasing until reaching the desired value. In this work, we stop at 15 hidden layers and obtain an error over the test set of $\sim 10^{-2}$. One can goes further (more hidden layers), but is enough for the purpose of this work.

After checking the convergence of the parameters, we repeat the training with all the synthetic data. As an example, in Fig. 2 is plotted the scattering cross length calculated considering $\gamma = 2$ and $R = 2$ (blue full line). Then, it is provided to the neural network as an input, and it “predicts” the values $\gamma \approx 1.92$ and $R \approx 1.98$. Consequently, is plotted the scattering cross length computed with those values (red dashed line). We calculate the percentage relative difference

$$\frac{|\gamma - p_\gamma|}{\gamma} \approx 4.1\%, \quad \frac{|R - p_R|}{R} \approx 1.2\%, \quad (15)$$

where p_γ and p_R stands for the “predicted” values obtained by the neural network.

III. PREDICTION WITH NOISE

The trained neural network can predict accurate values of parameters when the input data has noise. It was generated synthetic data $l(k)$ and was added Gaussian white noise with different width. Therefore, it was plotted (Fig. 3) the noisy scattering cross length with its respective

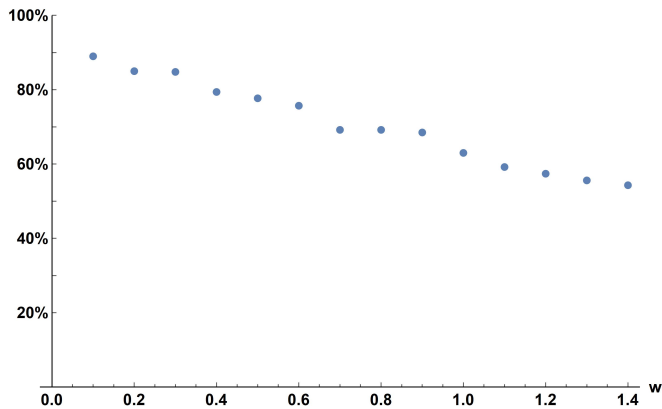


FIG. 4. Percentage of correct predictions for each noise width w . It is considered as a correct prediction any example with a percentage relative difference less than 10% for both parameters simultaneously.

prediction to elucidate the procedure. The four plots correspond to the same scattering cross length (same as presented at Fig.2), although their difference is the noise width. Along these lines, each example from Fig. 3 has

a correct prediction for the potential parameters. Here we consider a correct prediction as a percentage relative difference less than 10% for all the parameters. Then, it was generated one thousand of examples for each width of the noise, where the parameters were randomly selected between the interval $R \in [0.1, 2]$ and $\gamma \in [0.1, 3]$. In Fig. 3 is plotted the percentage of correct predictions for each noise width w . It is shown the decreasing of accurate predictions as the value of the noise increases.

IV. CONCLUSION

In this work we have shown how a simple neural network can predict correct values for potential parameters. We choose a circular boundary-wall potential due to the existence of the analytic solution for the wave function and the scattering cross length. However the vast majority of potential does not have an analytic solution for the wavefunction nor the scattering cross length (or scattering cross section in 3D problems). Consequently, one can obtain it via numeric (boundary integral methods) or approximate (Born approximation) methods. The neural network is able to determine the parameters even with a noisy input.

-
- [1] L. Mosser, O. Dubrule, and M. J. Blunt, Reconstruction of three-dimensional porous media using generative adversarial neural networks, *Phys. Rev. E* **96**, 043309 (2017).
 - [2] N. Kwak and Chong-Ho Choi, Input feature selection by mutual information based on parzen window (2002).
 - [3] S. Kamrava, P. Tahmasebi, M. Sahimi, and S. Arbabi, Phase transitions, percolation, fracture of materials, and deep learning, *Phys. Rev. E* **102**, 011001 (2020).
 - [4] E. d. M. Koch, A. d. M. Koch, N. Kastanos, and L. Cheng, Short-sighted deep learning, *Phys. Rev. E* **102**, 013307 (2020).
 - [5] R. A. Heinenon and P. H. Diamond, Turbulence model reduction by deep learning, *Phys. Rev. E* **101**, 061201 (2020).
 - [6] J. Zimmermann, B. Langbehn, R. Cucini, M. Di Fraia, P. Finetti, A. C. LaForge, T. Nishiyama, Y. Ovcharenko, P. Piseri, O. Plekan, K. C. Prince, F. Stienkemeier, K. Ueda, C. Callegari, T. Möller, and D. Rupp, Deep neural networks for classifying complex features in diffraction images, *Phys. Rev. E* **99**, 063309 (2019).
 - [7] R. A. Vargas-Hernández, Y. Guan, D. H. Zhang, and R. V. Krems, Bayesian optimization for the inverse scattering problem in quantum reaction dynamics, *New Journal of Physics* **21**, 022001 (2019).
 - [8] H. M. Yao, W. E. I. Sha, and L. Jiang, Two-step enhanced deep learning approach for electromagnetic inverse scattering problems, *IEEE Antennas and Wireless Propagation Letters* **18**, 2254 (2019).
 - [9] A. Palffy, J. Dong, J. F. P. Kooij, and D. M. Gavrilu, Cnn based road user detection using the 3d radar cube, *IEEE Robotics and Automation Letters* **5**, 1263 (2020).
 - [10] E. de Prunelé, Two-dimensional quantum scattering by non-isotropic interactions localized on a circle, applications to open billiards, *Journal of Mathematical Physics* **59**, 102102 (2018).
 - [11] A. C. Maioli and A. G. M. Schmidt, Exact solution to Lippmann-Schwinger equation for a circular billiard, *Journal of Mathematical Physics* **59**, 122102 (2018).
 - [12] A. C. Maioli and A. G. Schmidt, Exact solution to the Lippmann-Schwinger equation for an elliptical billiard, *Physica E: Low-dimensional Systems and Nanostructures* **111**, 51 (2019).
 - [13] A. C. Maioli and A. G. M. Schmidt, Two-dimensional scattering by boundary-wall and linear potentials, *Physica Scripta* 10.1088/1402-4896/ab57e6 (2019).
 - [14] M. G. E. da Luz, A. S. Lupu-Sax, and E. J. Heller, Quantum scattering from arbitrary boundaries, *Physical Review E* **56**, 2496 (1997).
 - [15] F. M. Zanetti, E. Vicentini, and M. G. da Luz, Eigenstates and scattering solutions for billiard problems: A boundary wall approach, *Annals of Physics* **323**, 1644 (2008).
 - [16] F. M. Zanetti, M. L. Lyra, F. a. B. F. de Moura, and M. G. E. da Luz, Resonant scattering states in 2D nanostructured waveguides: a boundary wall approach, *Journal of Physics B: Atomic, Molecular and Optical Physics* **42**, 025402 (2009).
 - [17] G. Rizzuti and A. Gisolf, An iterative method for 2d inverse scattering problems by alternating reconstruction of medium properties and wavefields: theory and application to the inversion of elastic waveforms, *Inverse Problems* **33**, 035003 (2017).

- [18] G. Ariel and H. Diamant, Inferring entropy from structure, *Phys. Rev. E* **102**, 022110 (2020).
- [19] T. Tyni, Numerical results for saito's uniqueness theorem in inverse scattering theory, *Inverse Problems* **36**, 065002 (2020).
- [20] G. Fotopoulos and M. Harju, Inverse scattering with fixed observation angle data in 2d, *Inverse Problems in Science and Engineering* **25**, 1492 (2017).
- [21] I. R. Lapidus, Quantummechanical scattering in two dimensions, *American Journal of Physics* **50**, 45 (1982).
- [22] P. A. Maurone and T. K. Lim, More on twodimensional scattering, *American Journal of Physics* **51**, 856 (1983).
- [23] S. K. Adhikari, Quantum scattering in two dimensions, *American Journal of Physics* **54**, 362 (1986), 1601.02657.
- [24] E. De Prunelé, Solvable quantum mechanical model in two-dimensional space, *Journal of Physics A: Mathematical and General* **39**, 12469 (2006).
- [25] J. Heaton, *Artificial Intelligence for Humans, Volume 3: Deep Learning and Neural Networks*, Artificial Intelligence for Humans (Createspace Independent Publishing Platform, 2015).
- [26] S. Fahlman and C. Lebiere, The cascade-correlation learning architecture, *Advances in Neural Information Processing Systems* **2** (1997).